QUANTIFICATION OF THE AIR BLAST CHARACTERISTICS OF COMMERCIAL EXPLOSIVES

S A Formby
Health and Safety Laboratory, Health and Safety Executive, Harpur Hill, Buxton, Derbyshire, SK17 9JN, UK

The pressure-time profiles produced by initiation in free-air of four commercial sector explosives covering a range of velocities of detonation are reported. The results indicate that there are no significant differences in the blast wave shapes from the explosives when measured between 5 and 20 m from the initiation point. The dependence of peak overpressure and positive phase impulse on scaled distance is presented, and compared to that of TNT. Analysis of peak overpressure and positive phase impulse data indicates that the TNT Equivalence of the explosives studied varies significantly with distance and method of calculation.

Key Words Airblast, TNT Equivalence, Explosion, Shock Wave, Explosive, Overpressure, Impulse, Damage.

INTRODUCTION

The UK Health and Safety Executive (HSE) has a need for tools to assist in the hazard evaluation of sites which pose an explosion risk, and also for models to aid post-accident assessments at such sites. These models enable prediction of damage at different distances from different sources and provide a means of estimating hazards both on site and beyond site boundaries.

In order to take account of the different damaging energy release from one explosive to another, the TNT Equivalence concept is widely used (1). Estimates of TNT Equivalence can be obtained by comparing the results from laboratory scale tests (such as the Ballistic Mortar and Lead Block Test) on explosives with data for TNT from the same methods. Another, more accurate, technique involves comparison of the well documented airblast characteristics (peak overpressure and positive phase impulse) for TNT with the effects produced from an equivalent weight of the explosive whose TNT Equivalence is to be determined.

There is evidence, as reported by De Yong and Campanella (2) and Swisdak (3), however, that blast parameters (e.g. peak overpressure, positive phase impulse) from different materials do not have the same distance-dependence as TNT. Also, the blast wave profiles from materials with slower energy release rates than TNT may exhibit different characteristics to those from TNT.

In order to examine the applicability of the TNT Equivalence model to airblast prediction, the Health and Safety Laboratory has undertaken research to measure the airblast characteristics from a range of detonating materials. A blast overpressure measurement facility has recently been constructed and commissioned at the Health and Safety Laboratory's site at Buxton to enable a detailed study to be undertaken in this area. Experiments to measure the peak overpressures and positive phase impulses at different distances from unconfined explosions in air of commercial explosives have been performed in order to compare them to TNT. This paper presents a preliminary analysis of the recorded blast waves.

EXPERIMENTAL DETAILS

A representative selection of commercial explosives was examined in order to cover a range of explosive strengths and detonation velocities. The four explosives studied were : Super Dopex; Powergel 700; Driftex; and Penobel 2. Table 1 gives further details.

Thin-walled frangible spherical plastic shells (of a design shown in Figure 1) were used to contain the explosives. Preliminary work was carried out to compare the blast from explosives contained in plastic bags with the blast from similar quantities of explosives contained in thin-walled frangible spheres. The results indicated that the plastic spheres had no significant effect on the resultant blast waves.

In order to enable measurement of the repeatability of recorded blast waves, five similar charges were prepared for each explosive. Each charge was produced by removing the explosive from its transport packaging, and pressing it into each half of a plastic sphere, leaving as few air spaces as possible. The filled hemispheres were then fitted securely together.

On reaching the test site, a Nobel No.6 detonator was inserted into the charge through a hollow plastic tube located in the top of the sphere. The charge was then suspended by thin netting and hoisted to 5m above the ground before initiation.

Blast waves from the following explosive charges were recorded : 0.9kg Super Dopex; 3.6kg Powergel 700; 4.9kg Driftex; and 3.8kg Penobel 2.

Pressure measurements were made with twelve Meclec FQ-11c piezo-electric gauges mounted in B12 baffles. Signals from these gauges were amplified and recorded on a Nicolet 500 series datalogger. 12 bit samples were taken at a sampling rate of 1MHz.

Gauges were positioned at a height of 5m above the ground, at 5, 10, 20, 30 ,40, 50, 75, and 100m from the firing position, as shown in Figure 2.

ANALYSIS OF SHOCKWAVE CHARACTERISTICS

The expected form of an ideal shock wave in air from an unconfined high explosive is shown in Figure 3. It is characterised by an abrupt (essentially discontinuous) pressure increase at the shock front, followed by a quasi-exponential decay back to ambient pressure. A negative phase follows, in which the pressure is less than ambient, and oscillations between positive and negative overpressure continue as the disturbance quickly dies away. These further oscillations, being of low pressure difference, are not very important compared to the first positive phase, and usually are not examined.

The backslope of the positive phase of an ideal air blast wave is commonly fitted to the modified Friedlander equation, which is given (6) by :

$$P'(t) = P_0 + OP_{\max}\left(1 - \frac{t}{t_d}\right)e^{-\frac{bt}{t_d}} \qquad [1]$$

where b is a positive constant.

The fitting of equation [1] to the upper portion of the backslope of a blast wave can be used to partially compensate for the non-ideal nature of pressure gauge recordings, caused by their finite response time and the presence of noise. This technique (1,7) was used to obtain the peak overpressures quoted in this paper.

It was found that the positive phase of the pressure-time recordings from the gauges at distances greater than 20m from the initiation point were modified by the presence of a ground-reflected wave. Analysis of such modified recordings are not presented in this paper. In order to provide a meaningful comparison between the measured blast waves from commercial sector explosives and those published for TNT, only pressure waves which exhibited near ideal wave shapes were analysed to obtain values for OP_{max} and I^+. Hence the pressure recordings made at 5, 10 and 20m from the charge were used for the analysis presented here.

Figure 4 shows shock wave profiles from the four explosives studied in these tests. The profiles have been scaled vertically and horizontally by different factors for illustrative purposes. The finite rise times of the blast recordings shown in this figure are in good agreement with the transit time for a shock wave to pass across the active face of the pressure gauge (approximately 60 μs).

The values for OP_{max} and I^+ for those pressure recordings that exhibited shock wave behaviour were calculated and then Sachs' scaled to standard sea level conditions, using the relationships given by Kingery and Bulmash (8) :

$$Z = \frac{R}{W^{\frac{1}{3}}\left(\frac{P_0}{P_a}\right)^{\frac{1}{3}}} \qquad [2]$$

$$P = \frac{P'}{\left(\frac{P_a}{P_0}\right)} \qquad [3]$$

$$\zeta = \frac{I}{W^{\frac{1}{3}}\left(\frac{P_0}{P_a}\right)^{\frac{2}{3}}\left(\frac{T_0}{T_a}\right)^{\frac{1}{2}}} \qquad [4]$$

The method used to estimate OP_{max} was that previously reported by Kinney and Graham (1), and Ismail and Murray (7). If t in the modified Friedlander equation [1] is measured from the time of arrival of the blast wave, then when t is small, $\left(1-\frac{t}{t_d}\right) \rightarrow 1$, so $\frac{d(\ln(P'-P_0))}{dt} \rightarrow -\frac{b}{t_d}$. Hence the natural logarithm of the overpressure ($P'-P_0$) in a blast wave, plotted against time, should be a straight line after OP_{max}. Extrapolation to time = 0 will yield $\ln(OP_{max})$, and provide an estimate of OP_{max} at the arrival time of the blast wave. Peak overpressure values calculated by this method were then Sachs' scaled, using equation [3].

Figure 5 shows the dependence of peak overpressure on scaled distance for the explosives initiated in these trials.

The positive phase impulse (per unit area) is given by $I^+ = \int_{t_a}^{t_d} P'(t)dt$, and was calculated by numerical integration of the recorded blast waves using FAMOS software (9). Impulse values calculated by this method were then Sachs' scaled, using equation [4], and Figure 6 illustrates the dependence of scaled impulse on scaled distance for the explosives examined in this study.

CALCULATION OF TNT EQUIVALENCE

The TNT Equivalence (TNT_e) of a material is given (10) by :

$$TNT_e(\%) = 100 \times \left(\frac{W_{TNT}}{W_x}\right) \qquad [5]$$

where W_x = weight of explosive charge
W_{TNT} = weight of TNT producing the same peak overpressure, or positive impulse, at the same distance.

This was calculated for the recorded blast waves using the methods described by Maserjian and Fisher (11), and published TNT spherical airburst data (8). These methods for calculation of TNT Equivalence have also previously been used by Esparza (12).

TNT Equivalence by overpressure can be calculated from the following relationship:

$$[TNT_e]_{OP_{max}} = \left(\frac{Z_x}{Z_{TNT}}\right)^3 \qquad [6]$$

where Z_x = scaled distance from the explosive charge
Z_{TNT} = scaled distance from TNT producing the same OP_{max}.

In order to obtain the TNT Equivalence by impulse, $[TNT_e]_{I^+}$, using the method of Maserjian and Fisher (11) it was necessary to obtain the intersection point of a 45° construction line with the TNT impulse curve, yielded by a plot of ζ^+ against Z. In order to simplify calculation of the intersection point, it was found that published TNT airburst impulse data (8) when plotted on a log-log graph against Z could be adequately approximated by a straight line dependence in the region of interest. A linear regression line was fitted to the TNT impulse data at scaled distances between 2 and 30 $m.kg^{-1/3}$, yielding a gradient of -0.94 on a log-log graph against scaled distance.

COMPARISON OF TNT EQUIVALENCE FROM OVERPRESSURE AND IMPULSE

Figures 7 and 8 indicate that different values of TNT Equivalence are obtained from overpressure and impulse data. In order to investigate the relative magnitude of the two values, the ratio $\frac{[TNT_e]_{OP_{max}}}{[TNT_e]_{I^+}}$ was calculated for each experiment and the values plotted against Z, Figure 9.

The graph clearly shows that $[TNT_e]_{OP_{max}} > [TNT_e]_{I^+}$ for all of the explosives tested. Also, the values of TNT Equivalence obtained by overpressure and impulse differ increasingly as Z increases from 2 to 13 $m.kg^{-1/3}$, although more data are required to examine the trend to greater distances.

DISCUSSION AND CONCLUSIONS

The pressure recordings made during these experiments indicated that there was no significant difference in blast wave shape from explosives with different detonation velocities at distances greater than 5m from the charge. All of the blast waves in these experiments had achieved shock-wave profiles by the time they had propagated 5m from the source.

Only those recordings of blast waves which were unaffected by the ground-reflected wave were used in the calculation of TNT Equivalence for the explosives studied. This enabled direct comparison with published TNT spherical airburst data. The use of an airburst (rather than groundburst) configuration isolated the experiments from the additional variables

which are introduced in groundburst experiments, (e.g. the energy absorbed during crater formation, and the absorption coefficient of the ground.)

The airblast experiments performed in this study have enabled TNT Equivalence values to be calculated by peak overpressure and positive phase impulse for a range of commercial sector explosives. Table 2 summarises the TNT Equivalences obtained from this study. The significant difference between TNT_e values calculated from our data for Penobel 2, and the value obtained from ballistic mortar measurements (4), Table 1, may be due to the lower confinement of the material in these airblast trials. Penobel 2 is a permitted mining explosive which is designed to release its full energy only when confined.

Blast waves from a range of explosives having detonation velocities between 7700 and 2000 $m.s^{-1}$ have been examined in this study, extending the range of materials for which airblast TNT Equivalence has been published. The dependence of TNT_e on distance and method of calculation for all of these materials is in agreement with previously published data from other authors (2, 3) who have investigated the TNT_e of other selected explosives. For example, De Yong and Campanella (2) have published information indicating that the TNT Equivalences calculated by overpressure for a range of primary explosives and pyrotechnics vary with distance. Swisdak (3) has also reported that the TNT Equivalence of some high velocity of detonation explosives (e.g. Composition B, Composition C-4, Pentolite, and Tritonal) varies with distance and with the method of calculation.

The results reported in this paper indicate that the predicted damage to a structure may be significantly different depending on whether TNT Equivalence derived from peak overpressure or positive phase impulse data is used for the explosion source. Therefore, in order to obtain the most accurate damage estimate for a structure, both peak overpressure and impulse values need to be determined for the source.

The programme of air burst experiments underway at Buxton is currently being extended to encompass selected commercial sector energetic materials (those materials which pose an explosion hazard, but are not classified as explosives). The results obtained from these studies will enable a detailed examination to be made of both the applicability of TNT Equivalence to quantification of the airblast hazard from a range of detonating materials, and the general applicability of the above observations.

NOMENCLATURE

W	charge mass	(kg)
R	distance	(m)
t	time	(s)
t_a	arrival time of blast wave	(s)
t_d	positive phase duration	(s)
$P'(t)$	pressure at time t	(Pa)
$P(t)$	Sachs' scaled pressure at time t	(Pa)
P_a	ambient atmospheric pressure	(Pa)
P_0	standard atmospheric pressure	(101,300 Pa)
T_a	ambient air temperature	(K)
T_0	standard air temperature	(288 K)
OP_{max}	peak overpressure	(Pa)
I	impulse	(s.Pa)
I^+	positive phase impulse	(s.Pa)
I^-	negative phase impulse	(s.Pa)
Z	scaled distance	($m.kg^{-1/3}$)
ζ	scaled impulse	($s.Pa.kg^{-1/3}$)
TNT_e	TNT Equivalence	(%)
$[TNT_e]_{OP_{max}}$	TNT Equivalence derived from overpressure data	(%)
$[TNT_e]_{I^+}$	TNT Equivalence derived from positive phase impulse data	(%)

ACKNOWLEDGEMENTS

The author is grateful to Mr A J Barratt and Mr I M Howard for undertaking the experimental work, and to Mr A E Jeffcock for his work in commissioning the blast measurement facility.

This work is funded by the Health and Safety Executive, and is forming the basis of post-graduate studies under the supervision of Professor S T S Al-Hassani, Chair in High Energy-Rate Engineering at UMIST, and Dr R K Wharton, Head of Explosives Section at the Health and Safety Laboratory. Partial payment of the academic fees for post-graduate registration is also gratefully acknowledged from Reverse Engineering Limited.

REFERENCES

1. G. F. Kinney and K. J. Graham, 1962, Explosive Shocks in Air, 2nd ed., pp. 2 and 100-102, Springer-Verlag, New York.

2. L. V. De Yong and G. Campanella, 1989, Journal of Hazardous Materials 21, pp. 125-133, A Study of Blast Characteristics of Several Primary Explosives and Pyrotechnic Compositions.

3. M. M. Swisdak, Jr., 1975, Explosion Effects and Properties, Part 1: Explosion Effects in Air, NSWC/WOL/TR 75-116, Naval Surface Weapons Center, White Oak, USA.

4. J. Köhler and R. Meyer, 1993, Explosives, 4th ed., VCH, Weinheim.

5. A. Marshall, 1917, Explosives, Vol. 2: Properties and Tests, 2nd ed., p. 491, J A Churchill, London.

6. W. E. Baker, 1973, Explosions in Air, pp. 5, 57 and 64, University of Texas Press, USA.

7. M. M. Ismail and S. G. Murray, 1993, Propellants, Explosives, Pyrotechnics 18, pp. 11-17, Study of the Blast Wave Parameters from Small Scale Explosions.

8. C. N. Kingery and G. Bulmash, 1984, Airblast Parameters from TNT Spherical Air Burst and Hemispherical Surface Burst, ARBRL-TR-02555, US Army Armament Research and Development Center, BRL, Aberdeen Proving Ground, Maryland, USA.

9. FAMOS (Fast Analysis and Monitoring Of Signals) User's Manual, 1993, imc Mess-systeme GmbH, Berlin, Germany.

10. M. Held, 1983, Propellants, Explosives, Pyrotechnics 8, pp. 158-167, TNT-Equivalent.

11. J. Maserjian and E. M. Fisher, 1951, Determination of Average Equivalent Weight and Average Equivalent Volume and their Precision Indices for Comparison of Explosives in Air, NAVORD Report 2264, US Naval Ordnance Laboratory, White Oak, Maryland, USA.

12. E. D. Esparza, 1986, International Journal of Impact Engineering 4(1), pp. 23-40, Blast Measurements and Equivalency for spherical charges at small scaled distances.

TABLE 1 : Details of the explosives tested[a]

Explosive	Description	Velocity of Detonation ($m.s^{-1}$)	TNT Equivalence by ballistic mortar (%)	Density ($g.cm^{-3}$)
Super Dopex	92-94% Nitro-Glycerine (NG) gelatinised with 6-8% nitro-cellulose	7700 (Blasting Gelatine)[b]	98	1.6
Powergel 700	Slurry explosive	3500 - 4500	71[c]	1.14
Driftex	NG based gelatinous permitted mining explosive (P1)	2500 - 3500	57	1.55
Penobel 2	NG powder permitted mining explosive (P4/5)	2000	37	1.3

TABLE 2 : TNT Equivalence values of some commercial explosives

Explosive	$[TNT_e]$ by ballistic mortar (%)	$[TNT_e]_{OP_{max}}$ (Average) (%)	$[TNT_e]_{I^+}$ (Average) (%)
Super Dopex	98	130	76
Powergel 700	71[c]	69	40
Driftex	57	63	38
Penobel 2	37	21	12

[a] All information from Köhler and Meyer (4), unless otherwise indicated.
[b] Information from Marshall (5).
[c] % energy of TNT (calculated from the weight strength of ANFO).

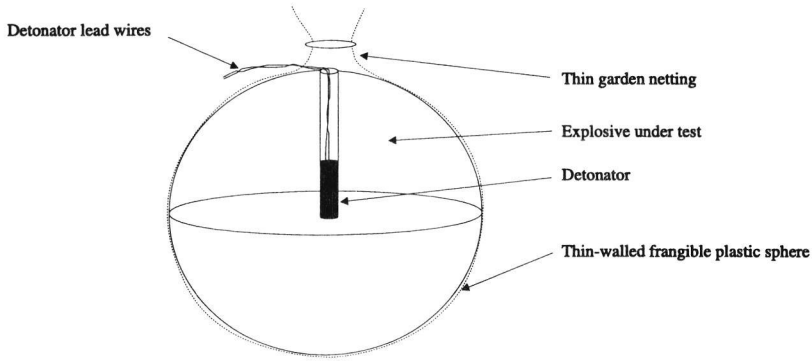

FIGURE 1 : Schematic of explosive charge

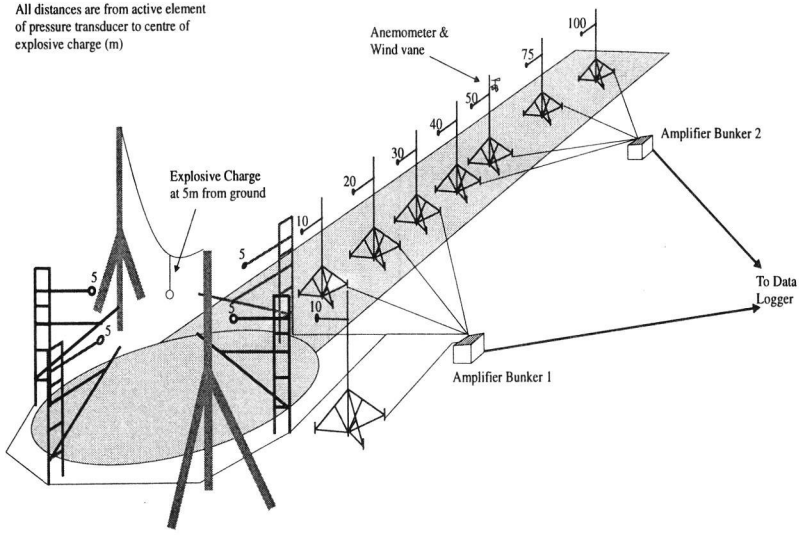

FIGURE 2 : Layout of blast range

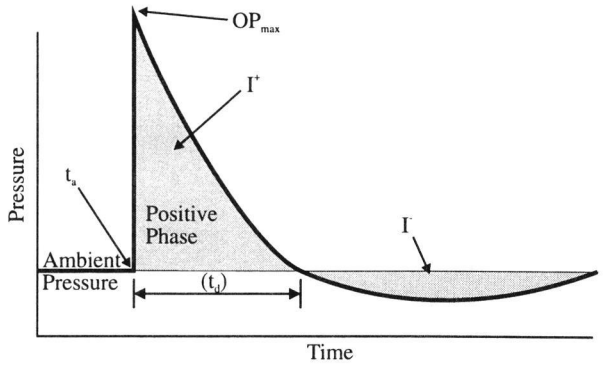

FIGURE 3 : Ideal shock wave in air

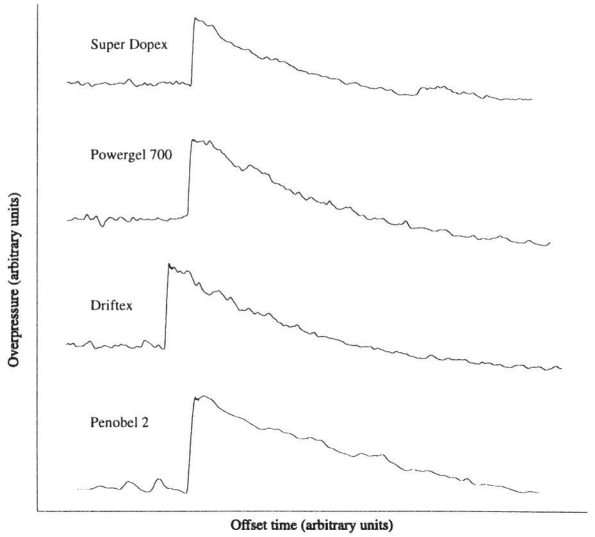

FIGURE 4 : Illustration of the similarity of pressure profiles recorded at 5m from the explosives studied

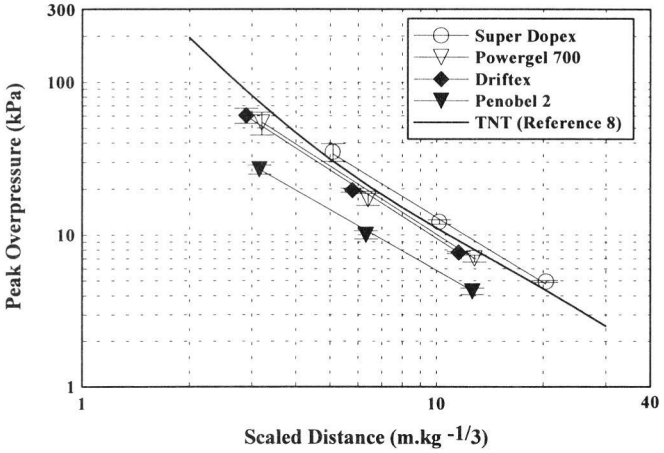

FIGURE 5 : The dependence of peak overpressure on scaled distance

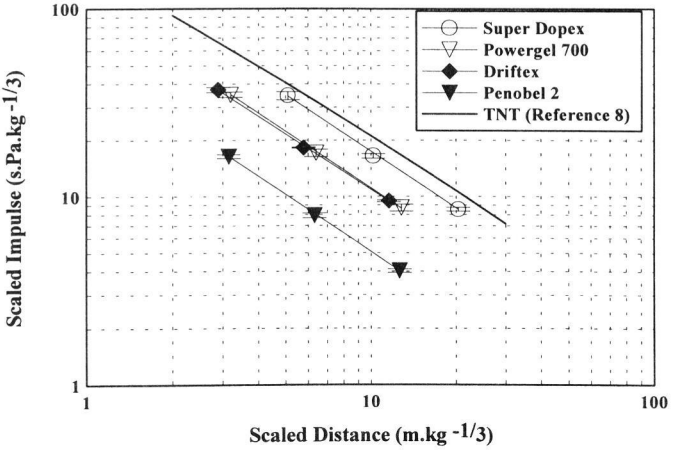

FIGURE 6 : The dependence of scaled impulse on scaled distance

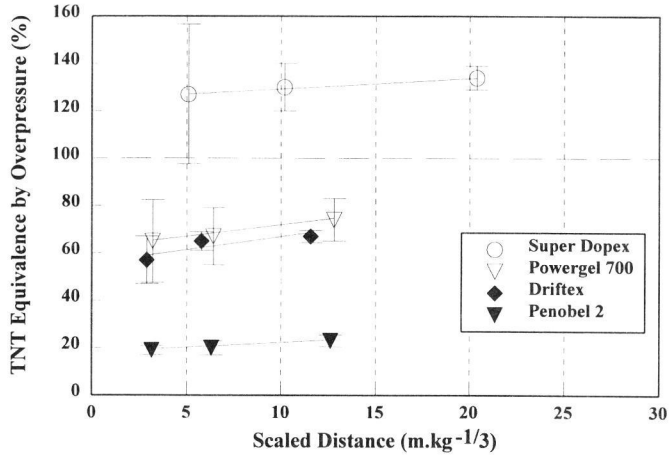

FIGURE 7 : The dependence of $[TNT_e]_{OP_{max}}$ on scaled distance

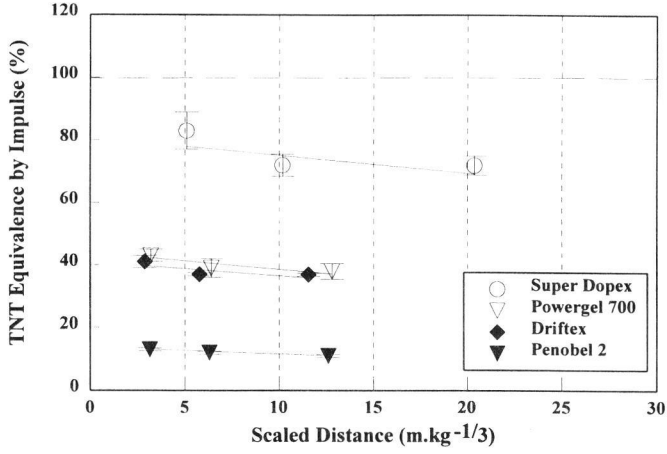

FIGURE 8 : The dependence of $[TNT_e]_{I^+}$ on scaled distance

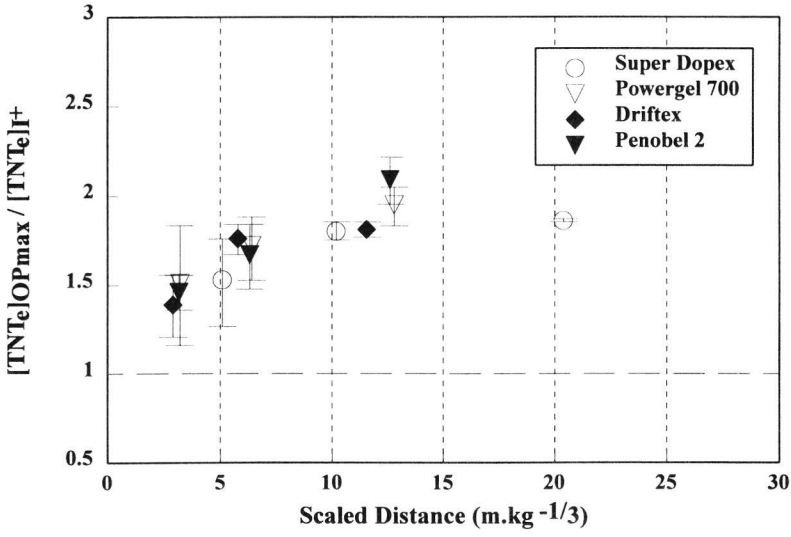

FIGURE 9 : The dependence of $\frac{[TNT_e]_{OP_{max}}}{[TNT_e]_{I^+}}$ on scaled distance